Front. Environ. Sci. Eng. 2021, 15(5): 106
https://doi.org/10.1007/s11783-021-1394-6

RESEARCH ARTICLE

Identification of resistant pharmaceuticals in ozonation using QSAR modeling and their fate in electro-peroxone process

Majid Mustafa (✉)[1*], Huijiao Wang [2*], Richard H. Lindberg[1], Jerker Fick[1], Yujue Wang (✉)[2], Mats Tysklind[1]

1 Department of Chemistry, Umeå University, Umeå S-90187, Sweden
2 School of Environment, Beijing Key Laboratory for Emerging Organic Contaminants Control, State Key Joint Laboratory of Environmental Simulation and Pollution Control (Ministry of Education), Tsinghua University, Beijing 100084, China

HIGHLIGHTS

- Effect of converting ozonation to E-peroxone was studied on pharmaceutical removal.
- A QSAR model was developed for selected 89 pharmaceuticals of special concern.
- Both processes abated the pharmaceuticals of moderate and high k_{O_3} quickly.
- E-peroxone process accelerated the elimination of pharmaceuticals with low k_{O_3}.
- Developed QSAR model reliably predicted k_{O_3} of 418 out of 491 pharmaceuticals.

GRAPHIC ABSTRACT

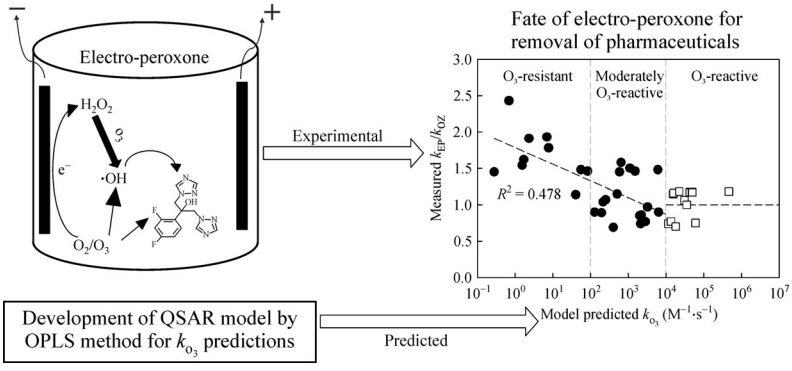

ARTICLE INFO

Article history:
Received 1 October 2020
Revised 13 December 2020
Accepted 18 December 2020
Available online 25 January 2021

Keywords:
Ozone
Electro-peroxone
Wastewater
Quantitative structure activity relationship
Advanced oxidation processes

ABSTRACT

The abatements of 89 pharmaceuticals in secondary effluent by ozonation and the electro-peroxone (E-peroxone) process were investigated. Based on the results, a quantitative structure-activity relationship (QSAR) model was developed to explore relationship between chemical structure of pharmaceuticals and their oxidation rates by ozone. The orthogonal projection to latent structure (OPLS) method was used to identify relevant chemical descriptors of the pharmaceuticals, from large number of descriptors, for model development. The resulting QSAR model, based on 44 molecular descriptors related to the ozone reactivity of the pharmaceuticals, showed high goodness of fit (R^2 = 0.963) and predictive power (Q^2 = 0.84). After validation, the model was used to predict second-order rate constants of 491 pharmaceuticals of special concern (k_{O_3}) including the 89 studied experimentally. The predicted k_{O_3} values and experimentally determined pseudo-first order rate constants of the pharmaceuticals' abatement during ozonation (k_{OZ}) and the E-peroxone process (k_{EP}) were then used to assess effects of switching from ozonation to the E-peroxone process on removal of these pharmaceuticals. The results indicate that the E-peroxone process could accelerate the abatement of pharmaceuticals with relatively low ozone reactivity ($k_{O_3} < \sim 10^2\ M^{-1}\cdot s^{-1}$) than ozonation (3–10 min versus 5–20 min). The validated QSAR model predicted 66 pharmaceuticals to be highly O_3-resistant. The developed QSAR model may be used to estimate the ozone reactivity of pharmaceuticals of diverse chemistry and thus predict their fate in ozone-based processes.

1 Introduction

Real water (e.g., surface water and wastewater) can typically contain hundreds of organic micropollutants (OMPs) that have widely varying molecular structures and physicochemical properties (von Sonntag and von Gunten, 2012; Lee et al., 2013; Loos et al., 2013; Li et al., 2014; Zhao et al., 2016). Ozonation is one of the most

✉ Corresponding authors
E-mail: majid.a.mustafa@umu.se (M. Mustafa);
wangyujue@tsinghua.edu.cn (Y. Wang)
*Co-first authors

studied treatment processes which has shown effective removal for large number of OMPs from wastewater effluents (Huber et al., 2003; Huber et al., 2005; Dodd et al., 2006; von Sonntag and von Gunten, 2012). Ozonation has also shown incomplete removal of many persistent OMPs due to selective nature of ozone (O_3) (Huber et al., 2003; Lee et al., 2013). Thus, there is a need of upgrading ozonation for better removal of structurally diverse and persistent OMPs.

The electro-peroxone (E-peroxone) process is an emerging ozone-based electrochemical advanced oxidation process (EAOP) that has shown great potential for removing emerging OMPs from contaminated water and wastewater (Yao et al., 2016; Yao et al., 2017; Wang et al., 2018b; Yao et al., 2018). It involves electrochemically produced hydrogen peroxide (H_2O_2) from cathodic oxygen (O_2) reduction during ozonation to enhance the transformation of O_3 to hydroxyl radicals (•OH). The enhanced formation of hydroxyl radicals can improve removal of OMPs that are resistant to O_3 oxidation (e.g., ibuprofen, clofibric acid, and chloramphenicol) compared to ozonation (Yao et al., 2016; Wang et al., 2018a; Yao et al., 2018; Li et al., 2021). In addition, unlike the conventional peroxone (O_3/H_2O_2) process which requires use of H_2O_2 stocks during ozonation, the E-peroxone process can produce H_2O_2 in situ by using O_2 that is always present in excess in ozonation. E-peroxone shows advantages in treatment window over ozonation, and therefore there is an argument for moving to this process. However, before widely applying the E-peroxone process in practice, systematic evaluation of the effects of changing from ozonation on abatement of a wide spectrum of OMPs is needed. Previous studies have compared the abatement of some OMPs by conventional ozonation and the E-peroxone process (Yao et al., 2016; Yao et al., 2017; Wang et al., 2018a; Yao et al., 2018; Li et al., 2019; Wang et al., 2019). The results suggest that the effects may depend on the OMPs' ozone reactivity. For example, the E-peroxone process reportedly eliminates ozone-resistant ibuprofen and chloramphenicol more strongly than ozonation, but may be less effective for eliminating bezafibrate, which is moderately O_3-reactive (Yao et al., 2016; Wang et al., 2018a). Given these differences in responses, and the small numbers of model OMPs tested in previous studies (Yao et al., 2016; Wang et al., 2018a; Yao et al., 2018), further clarification and generalization of the relationship between OMPs' ozone reactivity and their fates in the E-peroxone process is required.

The ozone reactivity of OMPs can be judged from the second-order rate constants of their reaction with O_3 (k_{O_3}). However, k_{O_3} values for many OMPs are still unknown. Experimentally measuring the k_{O_3} for each OMP is prohibitively expensive and practically infeasible. A practical alternative is to estimate k_{O_3} by using various computer based prediction approaches. One such approach is quantum chemical molecular orbital calculations for predictions of k_{O_3}. Lee et al. (2015) developed quantum chemical based models for aromatic compounds, olefins, and amines which correlated well with the energy of a delocalized molecular orbital on the aromatic ring, the energy of a localized molecular orbital in the carbon-carbon π bond, and the energy of the nitrogen lone-pair electrons on amines, respectively. However, these models are group specific local models with constrains in their applicability domains (Lee et al., 2015). Alternatively, the k_{O_3} can also be predicted by quantitative structure-activity relationship (QSAR) models based on a multitude of physico-chemical descriptors capturing molecular features related to reactivity. Such models are based on the thoroughly validated assumption that molecules' chemical reactivity is intrinsically linked to their structures and properties (Lei and Snyder, 2007; Jin et al., 2014; Jin et al., 2015; Borhani et al., 2016; Ortiz et al., 2017). For example, a univariate mechanistic QSAR model reported good correlation between k_{O_3} and the Hammett constants (σ) and Taft constants (σ^*) for aromatics and olefins, respectively (Lee and von Gunten, 2012). However, applicability domain of such models might be limited by the few available Hammett and Taft constants and complexity of the structures. QSAR models are also developed based on several physico-chemical properties by using a multiple linear regression (MLR) approach and have shown strong correlation with k_{O_3} (Sudhakaran et al., 2012). However, MLR can not handle inter-correlation between large number of physico-chemical properties (descriptors) and thus requires correlation analysis. In addition, descriptors also require separate assessment securing orthogonality by e.g., principal component analysis (PCA) (Sudhakaran et al., 2012). To overcome challenges in MLR, projections to latent structures by means of the partial least squares (PLS) method has been adopted. PLS is capable of analyzing many, collinear and noisy physico-chemical properties in relation to one or several response variables (Eriksson et al., 2006). The possibility to use a battery of physico-chemical properties for PLS based QSAR models increases precision and applicability domain of the model as many facets of chemical structure can be described. However, the interpretation of PLS model with large number of descriptors is complex due to structured noise in descriptors as well as possible inclusion of descriptors not correlated to the response studied (Eriksson et al., 2006). This challenge can be solved by orthogonal-PLS (OPLS) which is an extension of PLS (Wold et al., 2001; Trygg and Wold, 2002).

OPLS was adopted to develop QSAR model in current work. OPLS has the ability not only to handle inter-correlation between descriptors, but importantly can also reduce the number of descriptors relevant (predictive) to the response variable. This can be achieved as OPLS separates the descriptors into one part predictive to the

response (here: k_{O_3}) and an orthogonal part giving no predictive power and thus not explaining reactivity. This partitioning improves the model interpretability and transparency. Consequently, a large number of physico-chemical properties can be chosen initially to cover a broad range of structurally diverse OMPs and OPLS is used to identify the few most important predictive descriptors to k_{O_3}.

Thus, the main objective of this study was to explore the relationship between pharmaceuticals' ozone reactivity and their fate in ozone and E-peroxone process with support of QSAR modeling. A set of 89 pharmaceuticals of special concern for aquatic wildlife was selected to represent a broad range of relevant OMPs (Fick et al., 2010; Grabic et al., 2012), and a QSAR model was developed based on pharmaceuticals of known k_{O_3} to estimate unknown rate constants (k_{O_3}) of 491 pharmaceuticals including 89 in the target list. Special focus was on identifying recalcitrant pharmaceuticals and their characteristic physico-chemical features. The selected 89 pharmaceuticals were spiked in a secondary wastewater effluent and treated by ozonation and the E-peroxone process. Effects of upgrading ozonation to the E-peroxone process on removal of OMPs with varying ranges of ozone reactivity were then assessed. For this, we examined correlations between the k_{O_3} values predicted by the QSAR model and the experimentally determined pseudo-first order rate constants for abatement of the pharmaceuticals during ozonation (k_{OZ}) and the E-peroxone process (k_{EP}).

2 Materials and methods

2.1 Wastewater sample

A secondary wastewater effluent sample was collected from a municipal wastewater treatment plant in Beijing, China. The selected wastewater was stored at 4°C before it was used for oxidation experiments within 7 days of collection. Background concentrations of target pharmaceuticals in the wastewater were generally lower than their level of quantification (LOQ, see Supporting Information (SI) Table S1). To more accurately evaluate their abatements, appropriate volumes of pharmaceutical stocks (see SI Table S1 for names and structures of all studied 89 pharmaceuticals) were spiked in the selected wastewater (see SI Table S2 for water quality parameters) to obtain a nominal concentration of up to ~1 μg/L for each target pharmaceutical, which is generally within the typical concentration range of pharmaceuticals detected in wastewater. The detailed information of chemicals and reagents for this study can be found in SI Section S1.1, and the sample pre-treatment and analytical procedures of target pharmaceuticals are presented in SI Section S1.2 and Table S3.

2.2 Ozonation and the E-peroxone treatment

Semi-batch ozonation and E-peroxone treatments with continuous O_3 sparging were conducted in an undivided glass column reactor (250 mL, see SI Fig. S1) (Yao et al., 2016). During ozonation, O_3 was produced from pure O_2 (99.9%) feed gas using an ozone generator (OL80F/DST, Ozone Services, Canada). The ozone generator's effluent (O_2 and O_3 gas mixture) was then bubbled into the reactor at a 0.35 L/min flow rate controlled by a flow meter. Gas phase O_3 concentration at the reactor inlet and outlet were monitored using two ozone analyzers (BMT 964, Ozone Systems Technology International Inc., Germany) and used to calculate the amount of ozone consumed during treatment (see SI Section S2.1 for calculation details). Residual O_3 in the off-gas was decomposed using an ozone destructor. The reactor used for the E-peroxone process was equipped with a platinum anode (2 cm × 2 cm) and carbon-polytetrafluoroethylene (carbon-PTFE) cathode (5 cm × 2 cm). The ozone generator effluent (4.8 mg/L O_3, 0.35 L/min) was bubbled in the reactor in the same way as in conventional ozonation. Meanwhile, a constant current of 35 mA was applied using a DC power source to produce H_2O_2 from cathodic O_2 reduction. The molar ratio of O_3:H_2O_2 during the E-peroxone process was calculated based on the amounts of consumed O_3 doses and electro-generated H_2O_2 doses and found to be ~0.5–1.7 (see SI Fig. S2), which is generally within the range of O_3:H_2O_2 ratios often applied in conventional peroxone treatment of wastewater (e.g., O_3:H_2O_2 = 0.5–2) (Bourgin et al., 2017; Soltermann et al., 2017). All experiments were repeated twice in a water bath at 15°C±1°C.

2.3 Quantitative structure-activity relationship (QSAR) modeling

2.3.1 Data set of ozone rate constants and descriptors computation

To explore the intrinsic relationship between ozone reactivity and chemical structure, 30 of the set of 89 pharmaceuticals included in the analysis described above (see SI Table S1) with known k_{O_3} values were used for QSAR model development. Only a few of this set of 30 pharmaceuticals (e.g., fluconazole and oxazepam) have been reported as O_3-resistant compounds (with $k_{O_3} < 100\ M^{-1}\cdot s^{-1}$) (Lee et al., 2014). To cover the chemistry of O_3-resistant versus O_3-reactive compounds, balance the data set across a broad range of k_{O_3} values, and increase the applicability domain of the model, an additional 15 O_3-resistant pharmaceuticals (not included in the set of 89) with known reported k_{O_3} values were added for QSAR model development (see SI Table S4). Thus, in total, 45 pharmaceuticals with reported k_{O_3} were included in the initial QSAR modeling.

For descriptors computation, chemical structures of all pharmaceuticals were obtained from simplified molecular input line entry specification (SMILES). MOE (chemcomp.com) and Dragon (talete.mi.it) software packages were used to compute 2D and 3D chemical descriptors (as numeric values) from their structures (by SMILES codes). All structures were corrected for conformations by minimizing energies and partial charges were corrected by using the MMFF94-modified method (available in MOE) before calculating descriptor values.

As the starting point in the QSAR modeling, a set of 266 calculated descriptors were selected to cover the diverse physico-chemical properties (e.g., molecular, electronic, and steric properties) and effect of fragments of the pharmaceuticals. These included (*inter alia*) the octanol-water partition coefficient (log K_{ow}), molecular polarizability, aqueous solubility, van der Waals surface area, counts of specific atoms and bonds (single and aromatic bonds), molecular shape, number of donors/acceptors, polar positive/negative atoms in the structure, partial charges, potential energy descriptors, conformation and shape-dependent descriptors, dipole moment, and functional groups of the target pharmaceuticals.

2.3.2 QSAR model development and validation

To develop the QSAR model, the calculated physico-chemical descriptors (assigned as X-matrix) and available k_{O_3} of pharmaceuticals (assigned as Y-response) were imported to the SIMCA 16 multivariate statistical software package (Sartorius Stedim Data Analytics, Umeå, Sweden). The initial QSAR model was developed based on training set of 45 pharmaceuticals (N = 45) and 266 descriptors (K = 266) to screen predictive information of all 266 descriptors in relation to k_{O_3}. The orthogonal descriptors found by OPLS were removed due to irrelevance to k_{O_3}. Further, predictive descriptors that were adding more noise than predictive power were also removed by using variable (descriptor) influence on projection (VIP) parameter. Descriptors with VIP > 1.0 show highest predictive power while descriptors with VIP < 0.5 are responsible for noise with negligible predictive power thus removed except three. However, inclusion of descriptors with values ranging 0.5–1.0 and outlier pharmaceuticals were decided by model diagnostics such as R^2 (goodness of fit), Q^2 (internal validation), DmodX (observation distance to the model in the X space), DmodY (observation distance to the model in the Y space), VIP plot, and normal probability graphs to achieve the final model (SI Fig. S3 and Table S5) (Eriksson et al., 2006). The final refined QSAR model was based on training set of 40 pharmaceuticals (N = 40) (see SI Tables S1 and S4) and 44 chemical descriptors (K = 44) (see Table S6). The predictive power of the final QSAR model was validated with an external test set (see SI Tables S7 and S8) and collinearity by chance was investigated by a permutation test (randomizing response variable (k_{O_3}) by 100 iterations) (see SI Fig. S4).

3 Results and discussion

3.1 Pharmaceutical abatement by ozonation and the E-peroxone process

The abatement efficiencies of pharmaceuticals as a function of treatment time during ozonation and the E-peroxone treatment of the selected wastewater are shown in Fig. 1.

Among the tested 89 pharmaceuticals, 42 and 37 could be quickly abated to below their detection limits in the selected wastewater within 1 and 3 min of ozonation, respectively (Fig. 1(a)). However, elimination of 10 pharmaceuticals required at least 5 min or longer treatment time. In particular, fluconazole, which has a low O_3 rate constant of < 1 $M^{-1}\cdot s^{-1}$ and moderate •OH rate constant ($k_{\bullet OH}$) of 4.6×10^9 $M^{-1}\cdot s^{-1}$, was still detectable in the wastewater even after 20 min of ozonation.

During ozonation, OMPs are abated mainly by oxidation with O_3 and/or •OH generated from natural O_3 decomposition with •OH-generating water constituents such as phenols in dissolved organic matter (von Sonntag and von Gunten, 2012). Their abatement can usually be described by Eq. (1).

$$-\frac{d[P]}{dt} = k_{O_3}[O_3][P] + k_{\bullet OH}[\bullet OH][P]. \quad (1)$$

According to their O_3 rate constants (k_{O_3}), OMPs can be generally classified into three groups: 1) ozone-reactive ($k_{O_3} > 10^4$ $M^{-1}\cdot s^{-1}$), 2) moderately ozone-reactive ($100 < k_{O_3} < 10^4$ $M^{-1}\cdot s^{-1}$), and 3) ozone-resistant ($k_{O_3} < 100$ $M^{-1}\cdot s^{-1}$) (Lee et al., 2014; Zucker et al., 2016). While the k_{O_3} of various OMPs may vary over 8–10 orders of magnitude (e.g., from < 0.1 to $> 10^7$ $M^{-1}\cdot s^{-1}$), the $k_{\bullet OH}$ of most OMPs are not significantly different, typically varying within a factor of 3 in the range of 3×10^9 to 1×10^{10} $M^{-1}\cdot s^{-1}$ (von Sonntag and von Gunten, 2012). Therefore, OMPs with relatively high ozone rate constants can usually be more quickly abated than those with lower ozone rate constants during ozonation (von Sonntag and von Gunten, 2012; Yao et al., 2016; Guo et al., 2018).

This is consistent with patterns shown in Table 1. Previously published k_{O_3} values of pharmaceuticals that were eliminated within 1 min during ozonation generally exceeded 1.9×10^4 $M^{-1}\cdot s^{-1}$. Those of most of the pharmaceuticals eliminated in 1–3 min ranged from 1.7×10^3 to 1.9×10^4 $M^{-1}\cdot s^{-1}$ (with a few exceptions that were abated by > 89% in 1 min, e.g., paracetamol and clarithromycin, which have reported k_{O_3} values of 2.7×10^6 and 4.0×10^4 $M^{-1}\cdot s^{-1}$, respectively). Published k_{O_3}

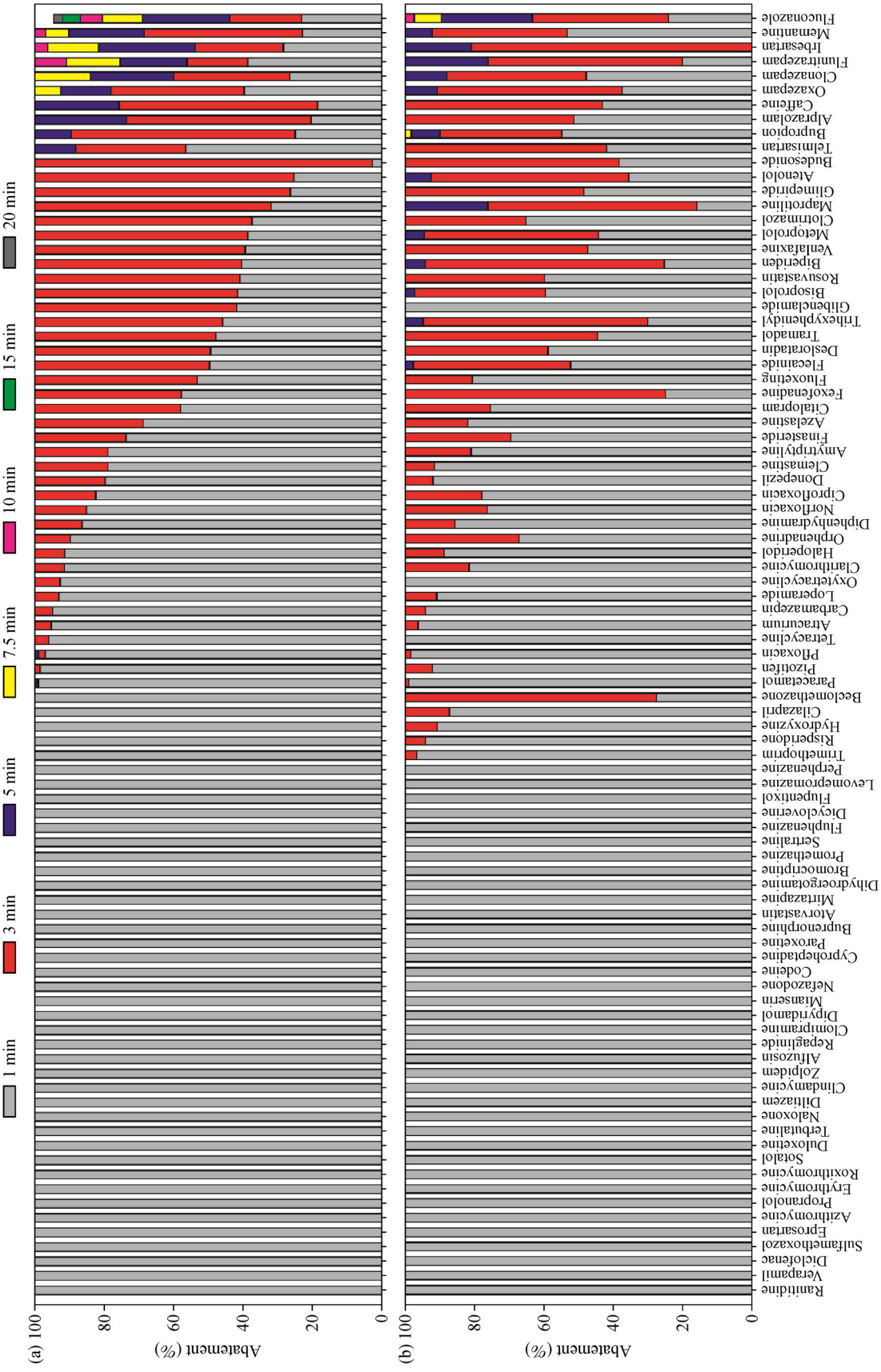

Fig. 1 Abatement of the selected set of 89 pharmaceuticals during (a) ozonation and (b) E-peroxone treatment of the selected wastewater. The pharmaceuticals are ordered from left to right along the *x*-axis in accordance with rapidity of their removal (highest to lowest). (Reaction conditions: volume = 250 mL, concentration of each pharmaceutical = ~1 μg/L, inlet O_3 gas phase concentration = 4.8 mg/L, gas flow rate = 0.35 L/min, current = 35 mA).

values of the pharmaceuticals that required ⩾5 min to eliminate are substantially lower: generally in the range of < 0.1–650 $M^{-1}\cdot s^{-1}$. The sole exception is telmisartan, which has a reported k_{O_3} of 1.2×10^5 $M^{-1}\cdot s^{-1}$ (Bourgin et al., 2018), but required 5 min of ozonation to eliminate (Fig. 1(a)). The reason for the slow abatement of telmisartan during ozonation is unclear, but may be due to its sorption to particles in the wastewater, which can provide some protection against ozone attack (Huber et al., 2005; Zucker et al., 2016).

The pharmaceuticals' abatement kinetics during the E-peroxone process differed in various ways (Fig. 1(b)). Most ozone-reactive and moderately reactive pharmaceuticals were quickly eliminated, within 1 and 3 min, respectively, as they were in ozonation. However, the E-peroxone process treatment time required to eliminate five fast-reacting and seven moderately-reacting pharmaceuticals was slightly higher (from 1 to 3 and 3 to 5 min ranges, respectively). These pharmaceuticals are trimethoprim, risperidone, hydroxyzine, cilazapril, beclomethazone, flecainide, trihexyphenidyl, bisoprolol, biperiden, metoprolol, maprotiline, and atenolol. In contrast, abatement of the 10 slow-reacting pharmaceuticals was considerably accelerated by the E-peroxone process, as it eliminated them more quickly from the wastewater (within 3–10 min) than ozonation (5–20 min). This acceleration can be mainly attributed to the faster decomposition of O_3 to •OH in the presence of electro-generated H_2O_2. Note that due to the mass transfer limitation of micropollutants to the anode surface, direct electrolysis usually plays a negligible role in micropollutant removal during the E-peroxone process (Wang et al., 2018a; Wang et al., 2019). OMPs with relatively low k_{O_3} values usually require longer reaction times to eliminate than those with higher k_{O_3}. Thus, the overall effect is that the hydraulic residence time required to abate the OMPs in real water matrices can be considerably shortened by shifting from ozonation to the E-peroxone process (see Fig. 1).

Due to its high efficiency for ozone-resistant micropollutant abatement, the E-peroxone process usually will not considerably increase, or can even reduce, the energy consumption for OMP abatement during water and wastewater treatment compared to ozonation (Yao et al., 2016; Yao et al., 2018). Consistently, Fig. 1 shows that ozonation and the E-peroxone process eliminated all spiked pharmaceuticals (with the only exception of fluconazole) in the selected wastewater in 10 and 5 min, when 2.57×10^{-5} and 2.80×10^{-5} kWh were consumed by the two processes, respectively (see SI Fig. S5). This result suggests that during the E-peroxone process, the extra energy demand for H_2O_2 electro-generation can be compensated by the reduced energy demand for O_3 generation; due to the enhanced •OH production from the reaction of O_3 with electro-generated H_2O_2, lower O_3 doses are generally required to abate O_3-resistant OMPs during the E-peroxone process than during ozonation (see SI Fig. S6 for discussion on pharmaceutical abatement as a function of consumed ozone dose).

Kinetic analysis indicates that the abatement of pharmaceuticals during both ozonation and the E-peroxone process can be generally described by pseudo-first order kinetics (Table 1). Note that the pseudo-first order rate

Table 1 pK_a values, previously published and QSAR model-predicted ozone rate constants (k_{O_3}), pseudo-first order rate constants obtained for abatement during ozonation (k_{OZ}) and the E-peroxone process (k_{EP}), and k_{EP}/k_{OZ} ratios for the tested pharmaceuticals

Compound	pK_a	k_{O_3} ($M^{-1}\cdot s^{-1}$)		$k_{\bullet OH}$ [b] ($M^{-1}\cdot s^{-1}$)	k_{OZ} (min^{-1})	k_{EP} (min^{-1})	k_{EP}/k_{OZ}
		Reported [a]	Predicted				
Alfuzosin			1.11×10^5				
Alprazolam			2.79×10^{-1}		0.458	0.662	1.45
Amitriptyline			2.53×10^2		1.554	1.657	1.07
Atenolol	9.6 [c]	1.7×10^3 [c]	2.24×10^3	8×10^9 [c]	1.004	0.865	0.86
Atorvastatin			1.63×10^4	1.19×10^{10} [d]			
*Atracurium			1.63×10^{11}		3.028	3.291	1.09
Azelastine			5.62×10^1		1.499	2.214	1.48
Azithromycin	8.7, 9.5 [e]	1.1×10^5 [e]	1.24×10^5	2.9×10^9 [e]			
Beclomethasone			2.49×10^3				
Biperiden			2.14×10^3		1.304	0.963	0.74
Bisoprolol			1.83×10^4		1.694	1.189	0.70
Bromocriptine			6.90×10^1				
Budesonide			5.10×10^2		0.508	0.583	1.15
Buprenorphine			1.70×10^5				
Bupropion			2.16×10^2	3.3×10^9 [f]	0.779	0.808	1.04
Caffeine		6.5×10^2 [g]	5.9×10^2	5.9×10^9 [h]	0.490	0.709	1.45

(*Continued*)

Compound	pK_a	k_{O_3} ($M^{-1}\cdot s^{-1}$)		$k_{\bullet OH}$ [b] ($M^{-1}\cdot s^{-1}$)	k_{OZ} (min^{-1})	k_{EP} (min^{-1})	k_{EP}/k_{OZ}
		Reported [a]	Predicted				
Carbamazepine		3×10^5 [i]		8.8×10^9 [i]	2.959	2.828	0.96
Cilazapril			5.14×10^2			2.056	
Ciprofloxacin	6.2, 8.8 [e]	1.9×10^4 [e]	3.59×10^4	4.1×10^9 [e]	1.633	1.626	1.00
Citalopram			1.11×10^3		0.868	1.301	1.50
Clarithromycin	9.0 [c]	4.0×10^4 [c]	6.07×10^4	5×10^9 [c]	2.458	1.842	0.75
Clemastine			6.51×10^2		1.558	2.463	1.58
Clindamycin	7.6 [c]	4.3×10^6 [c]	4.97×10^5	10^{10} [c]			
Clomipramine			1.32×10^2				
Clonazepam			2.35		0.362	0.690	1.91
Clotrimazole			8.36×10^1		0.728	1.065	1.46
Codeine			4.82×10^4				
Cyproheptadine			1.87×10^2				
Desloratadine			4.07×10^1		0.904	1.033	1.14
Diclofenac	4.2 [i]	1×10^6 [i]		7.5×10^9 [i]			
Dicycloverine			5.06×10^3				
Dihydroergotamine			1.46×10^2				
Diltiazem	8.2, 12.9 [j]		5.65×10^5	8.3×10^9			
Diphenhydramine			3.27×10^3	5.42×10^9 [d]	1.993	1.942	0.97
*Dipyridamole			3.28×10^3				
Donepezil			1.67×10^6		1.590	2.523	1.59
Duloxetine	9.7		3.04×10^5	9.72×10^9 [f]			
Eprosartan		4.9×10^5 [k]	1.00×10^6				
Erythromycin	8.4 [c]	7.9×10^4 [c]	5.21×10^4	5×10^9 [c]			
Fexofenadine	9 [l]	9.0×10^3 [l]	2.26×10^4		0.860	1.016	1.18
Finasteride			1.97×10^2		1.334	1.185	0.89
Flecainide			1.17×10^4		1.714	1.261	0.74
Fluconazole		< 1 [c]	0.69	4.6×10^9 [c]	0.207	0.501	2.43
Flunitrazepam			1.70		0.300	0.487	1.62
Fluoxetine	8.7 [m]	2.5×10^4	6.14×10^3	8.4×10^9 [n]	0.974	1.439	1.48
*Flupentixol			1.68×10^7				
*Fluphenazine			3.24×10^7				
*Glibenclamide			5.77×10^3		0.625		
*Glimepiride			1.53×10^3		0.474	0.693	1.46
Haloperidol			6.39×10^3		2.440	2.190	0.90
*Hydroxyzine			2.87×10^3			2.376	
Irbesartan		2.4×10^1 [k]	6.99	10^{10}	0.326	0.631	1.93
Levomepromazine			2.07×10^7				
Loperamide			1.29×10^2		2.650	2.391	0.90
Maprotiline			4.03×10^2		0.765	0.525	0.69
Memantine			7.75		0.474	0.843	1.78
Metoprolol	9.7 [o]	2.0×10^3 [c]	1.37×10^4	7.3×10^9 [p]	1.268	0.980	0.77
Mianserin			6.31×10^2				
Mirtazapine			1.25×10^3				

(*Continued*)

Compound	pK_a	k_{O_3} ($M^{-1}\cdot s^{-1}$)		$k_{\bullet OH}$ [b] ($M^{-1}\cdot s^{-1}$)	k_{OZ} (min^{-1})	k_{EP} (min^{-1})	k_{EP}/k_{OZ}
		Reported [a]	Predicted				
Naloxone			7.06×10^4				
*Nefazodone			1.01×10^3				
Norfloxacin	8.8 [c]	1.9×10^4 [c]	3.14×10^4	5×10^9 [c]	1.900	2.007	1.06
Ofloxacin	7.9 [q]	1.95×10^6 [r]	4.70×10^5	4.2×10^9 [r]	3.480	4.103	1.18
Orphenadrine			2.84×10^3		2.272	1.759	0.77
Oxazepam		~1 [c]	1.55	9.1×10^9 [c]	0.518	0.797	1.54
*Oxytetracycline			1.48×10^6	6.96×10^9 [s]	2.606		
Paracetamol		2.57×10^6 [t]		4.94×10^9 [t]	4.472	4.635	1.04
Paroxetine			6.91×10^4	9.6×10^9 [f]			
*Perphenazine			3.75×10^6				
Pizotifen			6.44×10^3			2.545	
*Promethazine			1.67×10^6				
Propranolol	9.5 [c]	1×10^5 [c]	1.95×10^4	10^{10} [p]			
Ranitidine	8.2 [c]	4.1×10^6 [c]	2.01×10^7	10^{10} [c]			
Repaglinide			6.31×10^3				
Risperidone			2.25×10^3			2.828	
Rosuvastatin			5.02×10^4		0.785	0.918	1.17
Roxithromycin	9.2 [e]	6.3×10^4 [e]	3.88×10^4	5.4×10^9 [e]			
Sertraline			1.60×10^1				
Sotalol	9.4 [c]	1.9×10^4 [c]	6.06×10^4	$\sim 10^{10}$ [c]			
Sulfamethoxazole	5.6 [o]	5.5×10^5 [e]	1.72×10^5	5.5×10^9 [e]			
Telmisartan		1.2×10^5 [k]	4.29×10^4		0.702	0.823	1.17
Terbutaline	8.6 [u]		1.23×10^5	6.87×10^9 [j]			
*Tetracycline	3.3,7.7,9.7 [e]	1.9×10^6 [e]	1.63×10^6	7.7×10^9 [e]	3.205		
Tramadol	9.4 [c]	4.0×10^3 [c]	1.57×10^4	6.3×10^9 [v]	0.856	0.981	1.15
Trihexyphenidyl			2.02×10^3		1.192	1.008	0.85
Trimethoprim	3.2, 7.1 [o]	4.1×10^5 [c]	4.57×10^5	6.9×10^9 [e]		3.398	
Venlafaxine	9.4 [c]	8.5×10^3 [c]	1.60×10^4	10^{10} [c]	0.842	0.977	1.16
Verapamil	9.7 [c]	2.7×10^6 [c]	3.74×10^6	10^{10} [c]			
Zolpidem			1.01×10^3				

Notes: *Pharmaceuticals with distance to model larger than 1.5 (outliers), a) k_{O_3} is the apparent second-order rate constant of the indicated pharmaceutical with O_3 at pH 7 unless otherwise stated; b) $k_{\bullet OH}$ is the apparent second-order rate constant of the indicated pharmaceutical with •OH at pH 7 unless otherwise stated; c) (Lee et al., 2014); d) (Razavi et al., 2011); e) (Dodd et al., 2006); f) (Santoke et al., 2012); g) (Broséus et al., 2009); h) (Shi et al., 1991); i) (Huber et al., 2003); j) (Zhu et al., 2015); k) (Bourgin et al., 2018); l) (Borowska et al., 2016); m) (Zhao et al., 2017); n) (Lam et al., 2005); o) (Bourgin et al., 2017); p) (Benner et al., 2008); q) (Okeri and Arhewoh, 2008); r) (Rodríguezet al., 2013); s) (López-Peñalver et al., 2010); t) (Hamdi El Najjar et al., 2014); u) (Allen et al., 1998); v) (Zimmermann et al., 2012)

constants for pharmaceuticals that were eliminated within 1 min are not reported because insufficient data points are available for linear regression. Of the 43 pharmaceuticals for which k_{OZ} and k_{EP} values could be calculated, 28 pharmaceuticals have a larger k_{EP} than k_{OZ} ($k_{EP}/k_{OZ} > 1$, see Table 1), which indicates that their abatement will be enhanced when ozonation is changed to the E-peroxone process (Yao et al., 2016; Yao et al., 2017). However, the k_{EP}/k_{OZ} ratio is slightly < 1 for 14 pharmaceuticals, suggesting that their abatement may be decelerated by changing ozonation to the E-peroxone process.

The differences in pharmaceutical abatement kinetics between ozonation and the E-peroxone process can be attributed to the enhanced transformation of O_3 to •OH by electro-generated H_2O_2 (Wang et al., 2018a). As shown in SI Fig. S2(a), the electro-generation of H_2O_2 did not markedly enhance O_3 transfer during the E-peroxone process compared to ozonation, especially in the first 5 min when all pharmaceuticals had been abated to below their detection limits during the E-peroxone process (with the

only exception of fluconazole, see Fig. 1(b)). However, the electro-generation of H_2O_2 considerably accelerated the transformation of transferred O_3, resulting in significantly lower aqueous O_3 concentrations during the E-peroxone process than ozonation (see Fig. S2(b)). Besides enhancing O_3 decomposition, the reaction of H_2O_2 with O_3 produces •OH with a higher yield (~50%, i.e., 0.5 mol of •OH produced per mole O_3 consumed) than those from the reaction of O_3 with •OH-generating water constituents (e.g., 24%–43% for phenols, 8%–17% for alkoxybenzenes, and 15% for tertiary amines) (Flyunt et al., 2003; von Sonntag and von Gunten, 2012; Fischbacher et al., 2013). Therefore, the electro-generation of H_2O_2 considerably enhanced O_3 transformation and •OH production during the E-peroxone process compared to ozonation (Yao et al., 2017; Yao et al., 2018). Consistently, SI Fig. S7 shows that the time-integrated concentration of •OH (i.e., •OH exposure) increased at significantly higher rates during the E-peroxone process than during ozonation. This observation confirms that higher •OH concentrations are maintained during the E-peroxone treatment of the selected wastewater. Due to the enhanced O_3 transformation to •OH when ozonation was changed to the E-peroxone process, the •OH oxidation capacity (measured as •OH exposure) increased considerably at the expense of decreasing the O_3 oxidation capacity (measured as O_3 exposure) (see SI Fig. S7 and refer to (Wang et al., 2018a)). For ozone-resistant OMPs (e.g., $k_{O_3} < 100\ M^{-1}\cdot s^{-1}$), which are abated solely by •OH oxidation during ozone-based processes (von Sonntag and von Gunten, 2012), the increase of •OH oxidation capacity can enhance their abatement during the E-peroxone process (Yao et al., 2017; Wang et al., 2018a). In addition, the decrease in O_3 oxidation capacity will not usually affect abatement of ozone-reactive pollutants (with $k_{O_3} > 10^4\ M^{-1}\cdot s^{-1}$) because very small O_3 oxidation capacities are required for their elimination (Guo et al., 2018; Wang et al., 2018a). In contrast, OMPs with moderate ozone reactivity (e.g., $k_{O_3} = \sim 10^2$–$10^4\ M^{-1}\cdot s^{-1}$) are usually abated by a combination of oxidation with O_3 and •OH. Therefore, their abatement may be enhanced or decreased, depending on whether the decrease in O_3 oxidation capacity can be sufficiently compensated by the increase in •OH oxidation capacity during the E-peroxone process (Wang et al., 2018a). Overall, moderately ozone-reactive OMPs can be eliminated at relatively high kinetics by the E-peroxone process (Wang et al., 2018a), as shown in Fig. 1(b).

To roughly estimate effects of changing from conventional ozonation to E-peroxone process on the abatement of OMPs, a relationship was developed between literature reported k_{O_3} and experimentally measured k_{EP}/k_{OZ}, as shown in SI Figs. S8 and S9. It was found that E-peroxone process can substantially accelerate the removal (k_{EP}/k_{OZ} = ~1.5–2.5) of pharmaceuticals with low ozone reactivity, whereas no substantial acceleration (k_{EP}/k_{OZ} = ~1) was observed for ozone-reactive pharmaceuticals (see SI Fig. S9 for detailed discussion). However, this relationship was based on few compounds because ozone rate constants for most pharmaceuticals tested in this study are still unknown. Therefore, a QSAR model was developed to estimate the ozone rate constants of the pharmaceuticals to further explore the relationship between OMPs' ozone reactivity and their fate in ozonation and the E-peroxone process.

3.2 Development of QSAR model for ozone rate constants (k_{O_3}) estimation

3.2.1 QSAR model parameters

The final QSAR model based on 44 descriptors had a high goodness of fit (R^2 = 0.963) and good internal validation (Q^2 = 0.84, see SI Table S5). These results indicate that the developed model is robust and has high predictive power. The correlation between the literature-reported and QSAR model-predicted ozone rate constants (k_{O_3}) for the training set of 40 pharmaceuticals is shown in Fig. 2. The k_{O_3} values predicted by the model are generally within a factor of 3 of the literature-reported values (see SI Fig. S10), which is considered acceptable given the complex chemistry of ozone reactions and uncertainty in ozone rate constant measurements (Lee and von Gunten, 2012; Lee et al., 2015). In addition, during model validation, analysis showed that no collinearity by chance occurred in

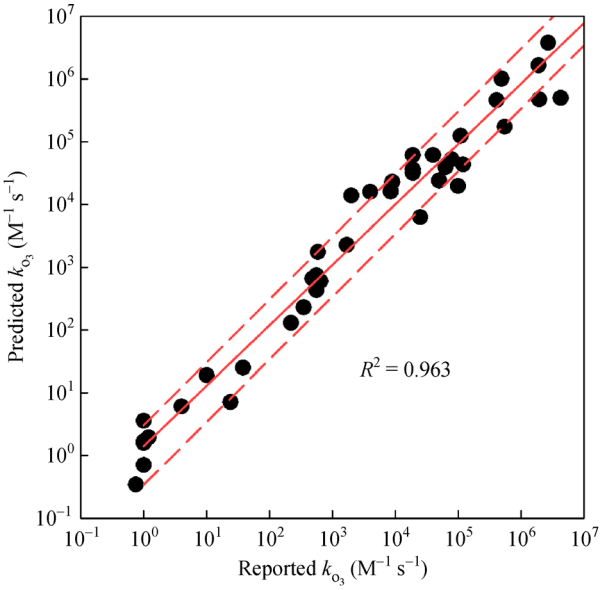

Fig. 2 Correlation between the literature-reported and QSAR model-predicted second-order rate constants for the reaction of O_3 with compounds used for model training. The solid line represents the linear regression line obtained, while the lower and upper dashed lines represent the prediction error ranges of factors of 1/3 and 3, respectively.

the data (shown in SI Fig. S4).

The second-order rate constants for the reaction of O_3 with the remaining 60 pharmaceuticals (with unknown k_{O_3} values) were then predicted using the developed QSAR model (see Table 1). The predicted k_{O_3} values for most pharmaceuticals that were quickly eliminated (within 1–3 min) during ozonation are in the range of 10^2–10^7 $M^{-1}\cdot s^{-1}$, while predicted values for pharmaceuticals that required > 5 min to eliminate are in the range of 10^{-1}–10^2 $M^{-1}\cdot s^{-1}$. The consistency between the predicted k_{O_3} values and experimentally observed abatement kinetics of pharmaceuticals shows that the model predicted the ozone reactivity of most pharmaceuticals tested in this study reasonably well.

However, several pharmaceuticals were quickly eliminated (within 1–3 min) during ozonation, but had low predicted k_{O_3} values, in the range 10^1–10^2 $M^{-1}\cdot s^{-1}$, for example, azelastine, bromocriptine, clomipramine, and sertraline (Fig. 1(a) and Table 1). This may be at least partly because the ozone reactivity of some moieties (e.g., phenolic and amine groups) in OMPs can be dramatically changed by protonation/deprotonation (Hoigné and Bader, 1983; von Sonntag and von Gunten, 2012). For example, deprotonation of phenolic and amine moieties can often increase OMPs' k_{O_3} values by ~4–6 orders of magnitude (von Sonntag and von Gunten, 2012). Depending on the solution pH and their pK_a, pharmaceuticals may be present in water mainly in either protonated or deprotonated forms, so their ozone reactivity may significantly vary. The QSAR model presented here estimates the k_{O_3} for the pharmaceuticals' molecular forms and does not consider the protonating/deprotonating effects of pH. This may account for at least some of the inconsistency between the low predicted k_{O_3} values and fast abatement kinetics observed for few pharmaceuticals during ozonation.

3.2.2 Physico-chemical properties related to k_{O_3}

The VIP plot (shown in Fig. 3) indicates importance of fraction of each variable in relation to k_{O_3}. Out of the final 44 descriptors (shown in Table S6), 24 and 20 were positively and negatively correlated with ozone reactivity (k_{O_3}), respectively. Detailed discussion on these correlated descriptors to k_{O_3} is provided in SI Section S2.9. Briefly describing, the most strongly negatively correlated descriptors, responsible for low O_3 reactivity, are electron withdrawing functionalities, partial charges descriptors, high lowest unoccupied molecular orbital energies, shape, and branching and atomic connectivity related descriptors. On the other hand, the most important positively correlated descriptors, associated with high ozone reactivity of pharmaceuticals (high k_{O_3}), include: the size-related variable, highest occupied molecular orbital energy, the conformation-dependent charge descriptors, surface area, diameter, and electron rich/donating moieties or functionalities.

3.3 Evaluation of pharmaceutical abatement by the QSAR model

Next, correlations between the k_{O_3} values predicted by the QSAR model and the experimentally determined k_{EP}/k_{OZ} ratios (Table 1) were examined to evaluate likely effects of switching from ozonation to the E-peroxone process on abatement of pharmaceuticals with varying ranges of ozone reactivity. As shown in Fig. 4, k_{EP}/k_{OZ} ratio generally decreases as the k_{O_3} of pharmaceuticals increases from 10^{-1} to 10^4 $M^{-1}\cdot s^{-1}$. This trend is similar to that observed in Fig. S9, which is plotted based on the literature-reported k_{O_3} of pharmaceuticals. Nevertheless, thanks to the model predicted k_{O_3}, more data points are

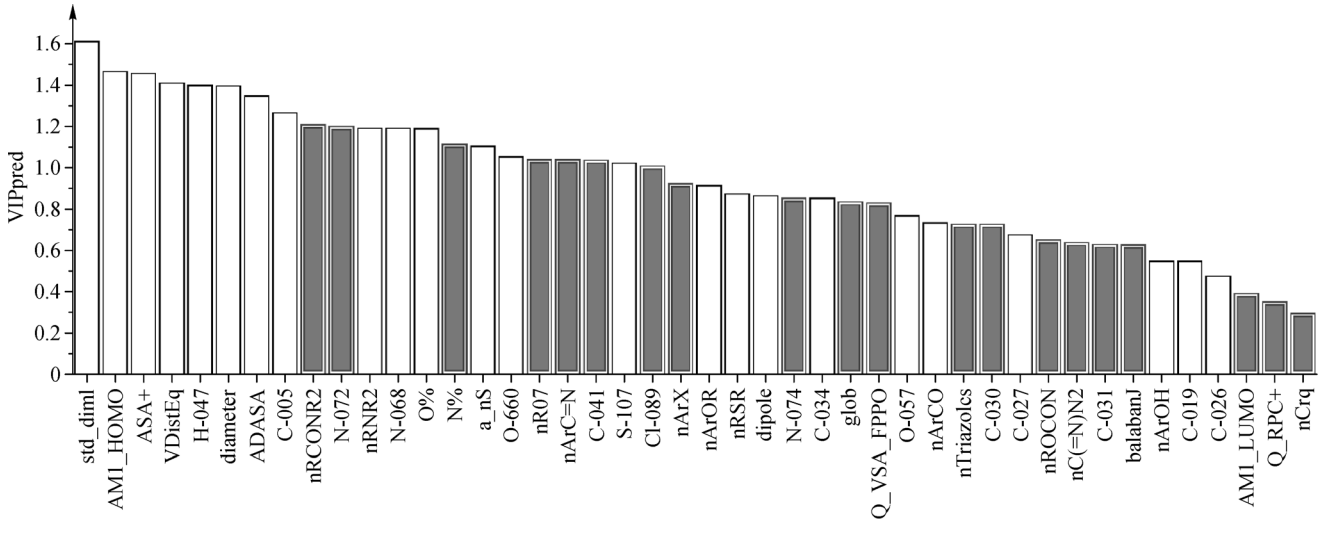

Fig. 3 VIP plot showing predictive descriptors (Table S6) in order from highest to lowest importance to k_{O_3}. Descriptors shown as white column bars were positively and descriptors as gray column bars were negatively correlated to k_{O_3}.

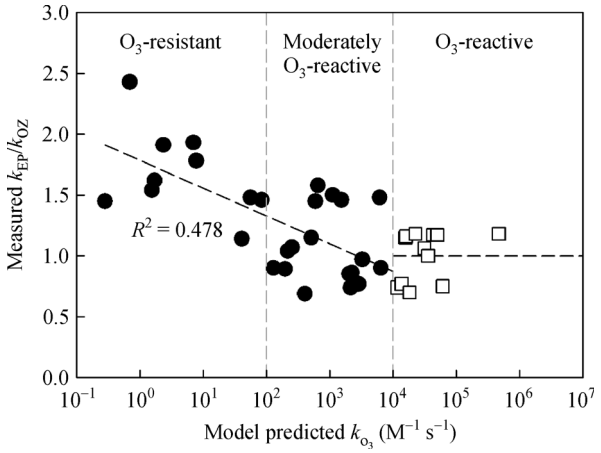

Fig. 4 The ratio of pseudo-first order rate constants for pharmaceutical abatement during the E-peroxone process and ozonation treatment (k_{EP}/k_{OZ}) in relation to the second-order rate constant for pharmaceutical reaction with ozone (k_{O_3}) predicted by the QSAR model.

available on Fig. 4 to more reliably elucidate the relationship between the ratio of k_{EP}/k_{OZ} of pharmaceuticals and their k_{O_3}. More specifically, for pharmaceuticals with $< 10^2$, 10^2–10^4 and $> 10^4$ $M^{-1}\cdot s^{-1} k_{O_3}$ values, the k_{EP}/k_{OZ} ratios are generally > 1.5, ~0.7–1.6 and ~0.8–1.2, respectively. These observations suggest that changing from ozonation to the E-peroxone process can accelerate the abatement of pharmaceuticals with relatively low ozone reactivity ($k_{O_3} < 10^2$ $M^{-1}\cdot s^{-1}$), especially those that are most resistant to O_3 oxidation ($k_{O_3} < 10$ $M^{-1}\cdot s^{-1}$). In contrast, the change will not substantially affect abatement of pharmaceuticals with moderate and high ozone reactivity, which were generally quickly eliminated during both processes (see Fig. 1).

Based on the results obtained for the 89 pharmaceuticals spanning a wide range of ozone reactivity ($k_{O_3} = \sim 10^{-1}$–10^7 $M^{-1}\cdot s^{-1}$), it can be concluded that ozonation is an effective process for abating OMPs with high and moderate ozone reactivity ($k_{O_3} > \sim 10^2$ $M^{-1}\cdot s^{-1}$). However, OMPs with low ozone reactivity ($k_{O_3} < \sim 10^2$ $M^{-1}\cdot s^{-1}$) are less efficiently eliminated during ozonation, which limits the overall efficiency of ozonation for OMP abatement in real water matrices. By generating H_2O_2 in situ from cathodic O_2 reduction to enhance O_3 transformation to •OH, the E-peroxone process can enhance abatement of O_3-resistant OMPs without compromising elimination of ozone-reactive and moderately reactive OMPs. Therefore, changing from conventional ozonation to the E-peroxone process is likely to improve overall abatement of OMPs in water and wastewater treatment.

3.4 Predictions of k_{O_3} and model applicability domain

To identify resistant pharmaceuticals, the established QSAR model was used to predict the second-order rate constants of 491 pharmaceuticals (including model compounds) of potential concern (see Table S9) (Fick et al., 2010). As many as 418 pharmaceuticals were inside the applicability domain of developed QSAR, as evaluated by their distance to model (DmodX) and shown in Fig. S11. Predictions outside of the QSAR model applicability domain (see Table S9 and Fig. S11) are extrapolations connected with high uncertainty. Table 2 presents the 66 O_3-resistant pharmaceuticals (excluding additionally added O_3-resistant pharmaceuticals for QSAR model development) showing $k_{O_3} < 100$ $M^{-1}\cdot s^{-1}$ as identified by the QSAR model and six compounds were located outside the model applicability domain.

Among O_3-resistant pharmaceuticals, two classes of pharmaceuticals stand out, viz. the benzodiazepines and the antifungal drugs. All benzodiazepines, drugs used to treat anxiety, included in this study appeared in O_3-resistant class. These second-generation cephalosporin antibiotics clearly indicate that the benzodiazepines have common chemical features less reactive toward ozone. A core chemical structure is the fusion of a benzene ring and a diazepine ring (a seven-membered ring structure with two nitrogen atoms), with chlorine or fluorine substituents on the benzene ring. All azole anti-fungal drugs were also in the O_3-resistant class ($k_{O_3} < 100$ $M^{-1}\cdot s^{-1}$). All these compounds have the azole-moiety in common, a five-member ring with two or three nitrogen, and similarly to the benzodiazepines, the azoles are halogenated. It is noteworthy that as many as 32 of the 66 pharmaceuticals in O_3-resistant class are aromatic halogenated. It should also be noted that even though antibiotics is the single, largest class of pharmaceuticals, only two were classified as O_3-resistant, i.e., streptomycin and loracarbef. Streptomycin, an aminoglycoside antibiotic, was extrapolated outside of model applicability domain, and loracarbef, a second-generation cephalosporin antibiotic, had a k_{O_3} of 96.9, just below the $k_{O_3} < 100$ $M^{-1}\cdot s^{-1}$ (see Table S9). For further interpretation of physico-chemical features, see Section 3.2.2.

Only few pharmaceuticals were predicted outside of the model domain showing low ozone reactivity as compared to those showing high ozone reactivity. This can be attributed to more specific chemistry of ozone resistant pharmaceuticals than ozone reactive pharmaceuticals that cover major proportion of the chemical space. In particular, all 491 pharmaceuticals were classified based on their QSAR model predicted k_{O_3} as shown in Fig. S11 (see Table S9 for predicted values of k_{O_3}). In total, 73 pharmaceuticals appeared in O_3-resistant class ($k_{O_3} < 100$ $M^{-1}\cdot s^{-1}$). The E-peroxone process is expected to accelerate the removal kinetics of these O_3-resistant pharmaceuticals by increasing transformation of O_3 into •OH as observed in experiments results. On the other hand, 214 and 204 pharmaceuticals appeared in the range of moderately O_3-

Table 2 The 66 O_3-resistant pharmaceuticals with $k_{O_3} < 100\ M^{-1}\cdot s^{-1}$ predicted by the QSAR model

Pharmaceutical	k_{O_3} ($M^{-1}\cdot s^{-1}$)	Pharmaceutical	k_{O_3} ($M^{-1}\cdot s^{-1}$)	Pharmaceutical	k_{O_3} ($M^{-1}\cdot s^{-1}$)
Ciclosporin	7.5×10^{-5}*	Ribavirin	6.58	Lomustine	42.1
Triazolam	0.0574	Praziquantel	6.60	Loratadine	47.6
Lorazepam	0.28	Irbesartan	6.99**	Dihydroergotamine	52.0
Alprazolam	0.28**	Ethosuximide	7.13	Guanethidine	55.0
Clobazam	0.67	Memantine	7.75**	Azelastine	56.2**
Fluconazole	0.69**	Felbamate	10.4	Itraconazole	60.8*
Anastrozole	1.23	Nitrazepam	13.0	Lisinopril	67.1
Oxazepam	1.55**	Zidovudine	15.2	Piperacillin	68.0
Letrozole	1.69	Sertraline	16.0**	Bromocriptine	69.0**
Flunitrazepam	1.70**	Methohexital	16.2	Mercaptopurine	80.7
Methenamine	2.0*	Levosimendan	16.9*	Domperidone	81.5
Clonazepam	2.35**	Phenobarbital	19.2	Clotrimazole	83.6**
Clonidine	2.52	Mitotane	20.7	Flucytosine	84.2
Carisoprodol	2.86	Moxonidine	20.9	Efavirenz	84.9
Amiloride	3.01	Dihydralazine	24.6	Baclofen	91.0
Amantadine	3.45	Chlordiazepoxide	29.3	Caspofungin	93.1*
Voriconazole	3.56	Streptomycin	29.3*	Gemcitabine	93.1
Proguanil	3.88	Melagatran	33.4	Nortriptyline	93.8
Artemether	4.75	Pyrimethamine	36.4	Oxcarbazepine	94.4
Pentobarbital	4.88	Ketamine	39.2	Quinaprilate	94.4
Midazolam	5.46	Desloratadine	40.7**	Alfentanil	96.2
Anagrelide	6.08	Isoflurane	41.9	Loracarbef	96.9

Notes: * Extrapolation outside of model applicability domain; ** OMP's also included in Table 1.

reactive (10^2–10^4 $M^{-1}\cdot s^{-1}$) and O_3-reactive ($k_{O_3} > 10^4$ $M^{-1}\cdot s^{-1}$) classes, which can generally be effectively abated in both ozonation and E-peroxone process. Considering the large number of O_3-resistant pharmaceuticals and other classes of OMPs, the E-peroxone process may be an appropriate choice for overall better removal of emerging contaminants.

4 Conclusions

Based on the comparison of abatement kinetics of a large set of pharmaceuticals during conventional ozonation and the E-peroxone process, it is now clear that shifting from ozonation to the E-peroxone process is likely to have differing effects on pharmaceuticals' abatement that are at least partly dependent on their ozone reactivities. Pharmaceuticals with moderate and high ozone reactivities ($k_{O_3} > 10^2$ $M^{-1}\cdot s^{-1}$) could typically be quickly eliminated by both processes. In contrast, the abatement of pharmaceuticals with low ozone reactivity ($k_{O_3} < 10^2$ $M^{-1}\cdot s^{-1}$) could be accelerated by the E-peroxone process. The acceleration varies, due to effects of diverse factors, but the shift is likely to be most beneficial for reducing levels of the most resistant pharmaceuticals. The VIP plot and model applicability domain plot clearly demonstrate that a combination of descriptors is needed to capture the chemical features related to ozone reactivity and increase the applicability domain of the QSAR model. The QSAR model showed high predictive capability and was able to identify a large set of pharmaceuticals for which special attention should be given in future studies of removal of OMPs from wastewater. Thus, the developed QSAR model appears to be a useful tool for estimating the ozone reactivity of OMPs and predicting their fate in ozonation and the E-peroxone process.

Acknowledgements This study was supported by the NSFC (Grant No. 51878370), the National Special Program of Water Pollution Control and Management (2017ZX07202), and the special fund of State Key Joint Laboratory of Environment Simulation and Pollution Control (18L01ESPC). The authors also thank the Industrial Doctoral School, Umeå University (Sweden), for financial support. The authors also acknowledge support from the Kempe Foundation (SJCKMS), Umeå University (Sweden) (for providing travel grants to conduct experiments at the School of Environment, Tsinghua University, Beijing, China), Ziye Zheng of Umeå University

(Sweden), for descriptors calculations, and Dr. David Andersson of Umeå University (Sweden), for valuable guidance in QSAR model development.

Electronic Supplementary Material Supplementary material is available in the online version of this article at https://doi.org/10.1007/s11783-021-1394-6 and is accessible for authorized users.

References

Allen R I, Box K J, Comer J E A, Peake C, Tam K Y (1998). Multiwavelength spectrophotometric determination of acid dissociation constants of ionizable drugs. Journal of Pharmaceutical and Biomedical Analysis, 17(4–5): 699–712

Benner J, Salhi E, Ternes T, von Gunten U (2008). Ozonation of reverse osmosis concentrate: Kinetics and efficiency of beta blocker oxidation. Water Research, 42(12): 3003–3012

Borhani T N, Saniedanesh M, Bagheri M, Lim J S (2016). QSPR prediction of the hydroxyl radical rate constant of water contaminants. Water Research, 98: 344–353

Borowska E, Bourgin M, Hollender J, Kienle C, Mcardell C S, von Gunten U (2016). Oxidation of cetirizine, fexofenadine and hydrochlorothiazide during ozonation: Kinetics and formation of transformation products. Water Research, 94: 350–362

Bourgin M, Beck B, Boehler M, Borowska E, Fleiner J, Salhi E, Teichler R, von Gunten U, Siegrist H, Mcardell C S (2018). Evaluation of a full-scale wastewater treatment plant upgraded with ozonation and biological post-treatments: Abatement of micropollutants, formation of transformation products and oxidation by-products. Water Research, 129: 486–498

Bourgin M, Borowska E, Helbing J, Hollender J, Kaiser H P, Kienle C, Mcardell C S, Simon E, von Gunten U (2017). Effect of operational and water quality parameters on conventional ozonation and the advanced oxidation process O_3/H_2O_2: Kinetics of micropollutant abatement, transformation product and bromate formation in a surface water. Water Research, 122: 234–245

Broséus R, Vincent S, Aboulfadl K, Daneshvar A, Sauvé S, Barbeau B, Prévost M (2009). Ozone oxidation of pharmaceuticals, endocrine disruptors and pesticides during drinking water treatment. Water Research, 43(18): 4707–4717

Dodd M C, Buffle M O, von Gunten U (2006). Oxidation of antibacterial molecules by aqueous ozone: Moiety-specific reaction kinetics and application to ozone-based wastewater treatment. Environmental Science & Technology, 40(6): 1969–1977

Eriksson L, Andersson P L, Johansson E, Tysklind M (2006). Megavariate analysis of environmental QSAR data. Part I–A basic framework founded on principal component analysis (PCA), partial least squares (PLS), and statistical molecular design (SMD). Molecular Diversity, 10(2): 169–186

Fick J, Lindberg R H, Tysklind M, Larsson D G (2010). Predicted critical environmental concentrations for 500 pharmaceuticals. Regulatory Toxicology and Pharmacology, 58(3): 516–523

Fischbacher A, von Sonntag J, von Sonntag C, Schmidt T C (2013). The OH radical yield in the $H_2O_2 + O_3$ (peroxone) reaction. Environmental Science & Technology, 47(17): 9959–9964

Flyunt R, Leitzke A, Mark G, Mvula E, Reisz E, Schick R, von Sonntag C (2003). Determination of •OH, $O_2^{\bullet -}$, and hydroperoxide yields in ozone reactions in aqueous solution. Journal of Physical Chemistry B, 107(30): 7242–7253

Grabic R, Fick J, Lindberg R H, Fedorova G, Tysklind M (2012). Multi-residue method for trace level determination of pharmaceuticals in environmental samples using liquid chromatography coupled to triple quadrupole mass spectrometry. Talanta, 100: 183–195

Guo Y, Wang H, Wang B, Deng S, Huang J, Yu G, Wang Y (2018). Prediction of micropollutant abatement during homogeneous catalytic ozonation by a chemical kinetic model. Water Research, 142: 383–395

Hamdi El Najjar N, Touffet A, Deborde M, Journel R, Karpel Vel Leitner N (2014). Kinetics of paracetamol oxidation by ozone and hydroxyl radicals, formation of transformation products and toxicity. Separation and Purification Technology, 136: 137–143

Hoigné J, Bader H (1983). Rate constants of reactions of ozone with organic and inorganic compounds in water—II: Dissociating organic compounds. Water Research, 17(2): 185–194

Huber M M, Canonica S, Park G Y, von Gunten U (2003). Oxidation of pharmaceuticals during ozonation and advanced oxidation processes. Environmental Science & Technology, 37(5): 1016–1024

Huber M M, Gobel A, Joss A, Hermann N, Loffler D, Mcardell C S, Ried A, Siegrist H, Ternes T A, von Gunten U (2005). Oxidation of pharmaceuticals during ozonation of municipal wastewater effluents: A pilot study. Environmental Science & Technology, 39(11): 4290–4299

Jin X, Peldszus S, Huck P M (2015). Predicting the reaction rate constants of micropollutants with hydroxyl radicals in water using QSPR modeling. Chemosphere, 138: 1–9

Jin X, Peldszus S, Sparkes D I (2014). Modeling ozone reaction rate constants of micropollutants using quantitative structure-property relationships. Ozone Science and Engineering, 36(4): 289–302

Lam M W, Young C J, Mabury S A (2005). Aqueous photochemical reaction kinetics and transformations of fluoxetine. Environmental Science & Technology, 39(2): 513–522

Lee M, Zimmermann-Steffens S G, Arey J S, Fenner K, von Gunten U (2015). Development of prediction models for the reactivity of organic compounds with ozone in aqueous solution by quantum chemical calculations: The role of delocalized and localized molecular orbitals. Environmental Science & Technology, 49(16): 9925–9935

Lee Y, Gerrity D, Lee M, Bogeat A E, Salhi E, Gamage S, Trenholm R A, Wert E C, Snyder S A, von Gunten U (2013). Prediction of micropollutant elimination during ozonation of municipal wastewater effluents: Use of kinetic and water specific information. Environmental Science & Technology, 47(11): 5872–5881

Lee Y, Kovalova L, Mcardell C S, von Gunten U (2014). Prediction of micropollutant elimination during ozonation of a hospital wastewater effluent. Water Research, 64(0): 134–148

Lee Y, von Gunten U (2012). Quantitative structure-activity relationships (QSARs) for the transformation of organic micropollutants during oxidative water treatment. Water Research, 46(19): 6177–6195

Lei H, Snyder S A (2007). 3D QSPR models for the removal of trace organic contaminants by ozone and free chlorine. Water Research, 41 (18): 4051–4060

Li X, Shi H, Li K, Zhang L, Gan Y (2014). Occurrence and fate of antibiotics in advanced wastewater treatment facilities and receiving rivers in Beijing, China. Frontiers of Environmental Science & Engineering, 8(6): 888–894

Li X, Wang B, Wang Y, Li K, Yu G (2019). Synergy effect of E-peroxone process in the degradation of structurally diverse pharmaceuticals: A QSAR analysis. Chemical Engineering Journal, 360: 1111–1118

Li Y, Zhang Y, Xia G, Zhan J, Yu G, Wang Y (2021). Evaluation of the technoeconomic feasibility of electrochemical hydrogen peroxide production for decentralized water treatment. Frontiers of Environmental Science & Engineering, 15(1): 1

Loos R, Carvalho R, António D C, Comero S, Locoro G, Tavazzi S, Paracchini B, Ghiani M, Lettieri T, Blaha L, Jarosova B, Voorspoels S, Servaes K, Haglund P, Fick J, Lindberg R H, Schwesig D, Gawlik B M (2013). EU-wide monitoring survey on emerging polar organic contaminants in wastewater treatment plant effluents. Water Research, 47(17): 6475–6487

López-Peñalver J J, Sánchez-Polo M, Gómez-Pacheco C V, Rivera-Utrilla J (2010). Photodegradation of tetracyclines in aqueous solution by using UV and UV/H_2O_2 oxidation processes. Journal of Chemical Technology and Biotechnology (Oxford, Oxfordshire), 85(10): 1325–1333

Okeri H A, Arhewoh I M (2008). Analytical profile of the fluoroquinolone antibacterials. I. Ofloxacin. African Journal of Biotechnology, 7(6): 670–680

Ortiz E V, Bennardi D O, Bacelo D E, Fioressi S E, Duchowicz P R (2017). The conformation-independent QSPR approach for predicting the oxidation rate constant of water micropollutants. Environmental Science and Pollution Research International, 24(35): 27366–27375

Razavi B, Ben Abdelmelek S, Song W, O'shea K E, Cooper W J (2011). Photochemical fate of atorvastatin (lipitor) in simulated natural waters. Water Research, 45(2): 625–631

, Rodríguez E M, Marquez G, Leon E A, Alvarez P M, Amat A MBeltran F J (2013). Mechanism considerations for photocatalytic oxidation, ozonation and photocatalytic ozonation of some pharmaceutical compounds in water. Journal of Environmental Management, 127: 114–124

Santoke H, Song W, Cooper W J, Peake B M (2012). Advanced oxidation treatment and photochemical fate of selected antidepressant pharmaceuticals in solutions of Suwannee River humic acid. Journal of Hazardous Materials, 217–218(0): 382–390

Shi X, Dalal N S, Jain A C (1991). Antioxidant behaviour of caffeine: Efficient scavenging of hydroxyl radicals. Food and Chemical Toxicology, 29(1): 1–6

Soltermann F, Abegglen C, Tschui M, Stahel S, von Gunten U (2017). Options and limitations for bromate control during ozonation of wastewater. Water Research, 116: 76–85

Sudhakaran S, Calvin J, Amy G L (2012). QSAR models for the removal of organic micropollutants in four different river water matrices. Chemosphere, 87(2): 144–150

Trygg J, Wold S (2002). Orthogonal projections to latent structures (O-PLS). Journal of Chemometrics, 16(3): 119–128

von Sonntag C, von Gunten U (2012). Chemistry of ozone in water and wastewater treatment: From basic principles to applications. London: IWA Publishing

Wang H, Mustafa M, Yu G, Ostman M, Cheng Y, Wang Y, Tysklind M (2019). Oxidation of emerging biocides and antibiotics in wastewater by ozonation and the electro-peroxone process. Chemosphere, 235: 575–585

Wang H, Zhan J, Yao W, Wang B, Deng S, Huang J, Yu G, Wang Y (2018a). Comparison of pharmaceutical abatement in various water matrices by conventional ozonation, peroxone (O_3/H_2O_2), and an electro-peroxone process. Water Research, 130: 127–138

Wang Y, Yu G, Deng S, Huang J, Wang B (2018b). The electro-peroxone process for the abatement of emerging contaminants: Mechanisms, recent advances, and prospects. Chemosphere, 208: 640–654

Wold S, Sjöström M, Eriksson L (2001). PLS-regression: A basic tool of chemometrics. Chemometrics and Intelligent Laboratory Systems, 58 (2): 109–130

Yao W, Qu Q, von Gunten U, Chen C, Yu G, Wang Y (2017). Comparison of methylisoborneol and geosmin abatement in surface water by conventional ozonation and an electro-peroxone process. Water Research, 108: 373–382

Yao W, Ur Rehman S W, Wang H, Yang H, Yu G, Wang Y (2018). Pilot-scale evaluation of micropollutant abatements by conventional ozonation, UV/O_3, and an electro-peroxone process. Water Research, 138: 106–117

Yao W, Wang X, Yang H, Yu G, Deng S, Huang J, Wang B, Wang Y (2016). Removal of pharmaceuticals from secondary effluents by an electro-peroxone process. Water Research, 88: 826–835

Zhao W, Guo Y, Lu S, Yan P, Sui Q (2016). Recent advances in pharmaceuticals and personal care products in the surface water and sediments in China. Frontiers of Environmental Science & Engineering, 10(6): 2

Zhao Y, Yu G, Chen S Y, Zhang S Y, Wang B, Huang J, Deng S B, Wang Y J (2017). Ozonation of antidepressant fluoxetine and its metabolite product norfluoxetine: Kinetics, intermediates and toxicity. Chemical Engineering Journal, 316: 951–963

Zhu B, Zonja B, Gonzalez O, Sans C, Perez S, Barcelo D, Esplugas S, Xu K, Qiang Z (2015). Degradation kinetics and pathways of three calcium channel blockers under UV irradiation. Water Research, 86: 9–16

Zimmermann S G, Schmukat A, Schulz M, Benner J, von Gunten U, Ternes T A (2012). Kinetic and mechanistic investigations of the oxidation of tramadol by ferrate and ozone. Environmental Science & Technology, 46(2): 876–884

Zucker I, Avisar D, Mamane H, Jekel M, Hübner U (2016). Determination of oxidant exposure during ozonation of secondary effluent to predict contaminant removal. Water Research, 100: 508–516